Solar wind as causative and coupling source of planetary atmospheres

R. N. Singh

Department of Applied Physics, Institute of Technology, Banaras Hindu University, Varanasi 221 005, India

The processes of solar wind generation and propagation have been reviewed. Relevant theoretical developments are given so as to analyse and interpret the observed planetary ionospheric and magnetospheric phenomena arising from solar wind interactions with inner planets, their moons and comets. The solar wind flux variations over a solar cycle have been described with a view to deciphering the induced global atmospheric phenomena from those of localized atmospheric origin. With the background of these details, the nature of solar wind interactions with the magnetic and non-magnetic planets and other objects can be easily analysed in term of physical knowledge of interacting targets. The study of solar wind interaction with solar system objects has assumed great importance as a probing tool and is capable of providing new information.

THE knowledge of the processes of generation and propagation of solar wind has become a key point in the correct understanding of the relationship between solar and planetary phenomena, in general, and some of the special planetary phenomena, in particular. The study of solar control on the earth's atmosphere has been systematically carried out for a long time on global scale and an adequate understanding of solar-terrestrial relationship has emerged which is illustrative of solar relationship with magnetic planets. Solar control on non-magnetic planetary atmospheres, their moons and comets are equally important but it has not been studied in detail so far. The purpose of this article is to set a needed perspective for readers to appreciate and understand the solar control on planetary plasma phenomena. The generation of solar wind and its propagation to planetary orbits has been discussed for benefit of those who wish to pursue the impact or interaction of solar wind on the planetary phenomena. A brief background of historical developments, selected theoretical details and some of the important associated features of solar wind have been described. The solar wind has been an important subject of numerous review papers and the intent of this paper is only to emphasize some of the solar wind aspects relevant for understanding and interpretation of the solar wind-induced planetary phenomena.

The discovery of solar wind and sources

The presence of plasma streams of corpuscular nature from the Sun and its qualitative effect has been known for many years[1]. Biermann[2,3] while studying the morphological details of extended Comets tail, for the first time, postulated the existence of solar wind. The generation process of solar wind remained unknown for quite sometime. Parker[4] tried to explain the Biermann's postulates, and later Chapman[5] suggested that the conduction of energy from the lower part of the solar corona is responsible for maintaining the interplanetary plasma stream at a temperature of 2×10^5 K near earth's orbit. Parker[4] demonstrated the generation mechanism of solar wind postulated by Biermann. He demonstrated the inevitability of the existence of steady state solar wind. Most of the solar wind models imply the role of the lower boundary of the solar corona where the plasma is hot. Chapman[5] suggested the lower part of the solar corona as a heat source from where conduction of energy takes place upwards and propagates through the diverging solar magnetic field configuration into the interplanetary space. Chamberlain[6,7] challenged Parker's ideas and claimed that the subsonic solutions of the hydrodynamical equations give rise to 'solar breeze' which satisfies the boundary condition of zero pressure at infinity. This solution is not representative of the actual state and physical characteristics of solar corona. The controversy was resolved in favour of the supersonic solar wind with the help of first direct space measurements of solar plasma flow with a velocity of 400 km sec^{-1}. The space probe measurements have shown that the solar wind plasma is emitted from the entire Sun. For a very long time, the variation of solar wind plasma flow from streamer to inter-streamer regions and the evolution of plasma flow during the build-up and decay periods of high speed solar wind region remained unknown. The coronal streamers are characteristic structures which arise from underlying solar magnetic field structures of a complex system of sunspots. Not much is yet known because of the inaccessibility of the region for *in situ* measurements The measurements and analyses of electromagnetic radiations are primary sources for obtaining detailed features of the solar wind emission region.

Various incompatibilities of earlier solar wind models and theories (based on these models) have come to light. Holloweg[8, 10] has replaced the simple heat conduction process of Chapman[5] by generation, transmission and attenuation of MHD waves. However, the MHD wave dissipation rate was found to be slow to account for the energy flux contained in the solar wind. Vanbeveren and de Loore[11] included the concept of enthalpy flow in the coronal heating by accounting for the dissipation of acoustic waves and formation of shocks. If enthalpy flow is important in the energy balance of the solar transition region and lower corona, then self-consistent treatment of solar wind should also satisfy the requirement that the plasma flow must pass through the critical point as envisaged by Parker[4]. Couturier *et al.*[12] and Souffrin[13] emphasized that the heating of the solar corona and generation of solar wind phenomenon are basically inter-related. However, it is generally believed that the observed coronal motion alone is not adequate to carry out the required energy fluxes to 1 AU and beyond, if the heating source is the dissipation of sound waves or acoustic shock trains alone. The coronal holes are well-known sources of high speed solar wind plasma streams[14-16]. The large mass flow from the photospheric region surrounding the foot of the magnetic field configuration into the coronal hole region increases the enthalpy flux of the transition region and enhances the solar wind speed that may continue to affect planetary phenomena for several solar rotations.

The source characteristics of solar wind can be considered in two distinct groups namely:

i) Distances within $10\,R_s$ – For solar wind propagating out to less than $10\,R_s$, the electron heat conduction process holds good and provides adequate energy to solar wind.

ii) Distances beyond $10\,R_s$ – The background plasma in regions beyond $10\,R_s$ is collisionless which satisfies the condition $R_s \to \infty$, $T \to 0$. These inner and outer interplanetary regions are connected discontinuously because of the characteristic change from collisional to collisionless regimes prevailing near and far from the Sun. The change from collisional to collisionless feature of interplanetary space results into a coronal temperature profile which is quite realistic[9, 17]. These models are not realistic and are less amenable to global heating as shown by Olbert[18] and Scudder and Olbert[19].

Following the *in situ* measurements of solar wind at 1 AU, Holloweg accounted for dissipation of Alfvèn waves which, as before, also implies that the coronal heating occurs below the base of the solar corona. An expression for plasma volumetric heating rate was obtained to show the nature of solar wind emission from the 'coronal holes'. This model does explain some of the unexplained features but fails to account for some of the observed features of the solar wind especially between the transition region within the solar atmosphere and extending up to 1 AU.

Theories of solar wind

Hydrodynamic theory: single fluid model

Parker proposed the expansion of solar coronal plasma in the form of solar wind as a natural consequence of high temperature solar corona. The hydrodynamic model of solar wind was postulated on the basis of the following assumptions: (i) single component fluid model, (ii) scalar solar coronal pressure; (iii) inviscid and spherically symmetric solar corona, and (iv) non-rotating and steady state solar corona.

The solution of equation of motion and continuity equation of the solar plasma in response to high temperature prevalent in the solar corona was the first step in understanding primary features of solar wind. At the base of the solar corona $r = a$, the temperature of the plasma is governed by Maxwellian distribution and $T_{(r=a)} = T_0$. This condition defines the 'critical point' at which the radial solar wind velocity is

$$V_r = (kT_r / \mu m_H)^{1/2}, \tag{1}$$

where μ is the mean molecular weight and m_H is the mass of the hydrogen atom. The velocity is close to the velocity of sound waves which is written as

$$V_{\text{sound}} = \left[\frac{\gamma P}{\rho}\right]^{\frac{1}{2}} = \left[\frac{5}{3}\frac{kT_r}{\mu m_H}\right]^{\frac{1}{2}}. \tag{2}$$

Far away from the Sun, we find that the radial velocity of the solar wind changes logarithmically. This implies that the thermal region must be terminated at some finite distance from the Sun. The variation of radial solar wind velocity V_s with r/R_s is shown in Figure 1. The solar wind velocity is seen to increase rapidly in the vicinity of the Sun and depends on the heat source and heat conduction processes. Another important parameter of the solar wind is the proton density and the solar wind flux nv_s. With initial success, the hydrodynamic theory is found to be adequate in explaining various observed features of solar wind. Some of the weaknesses of this theory are:

(i) This theory yields a higher density at 1 AU compared to *in situ* measured proton density.
(ii) The form of the solution and nature of the solar wind depends on the selection of integration constant which is governed by the solar coronal conditions which are known to change from time to time.

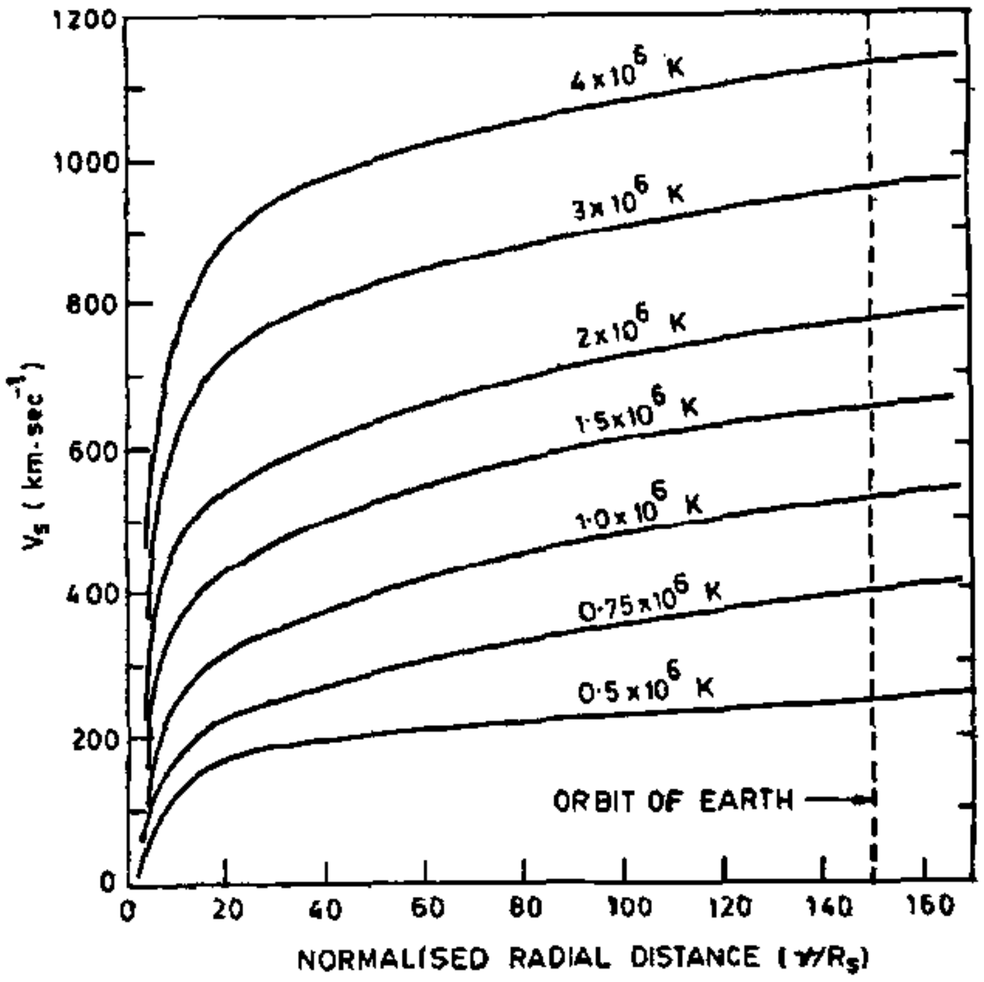

Figure 1. Variation of solar wind velocity with normalized radial distance computed from Parker's solar wind equations for different temperature of the corona

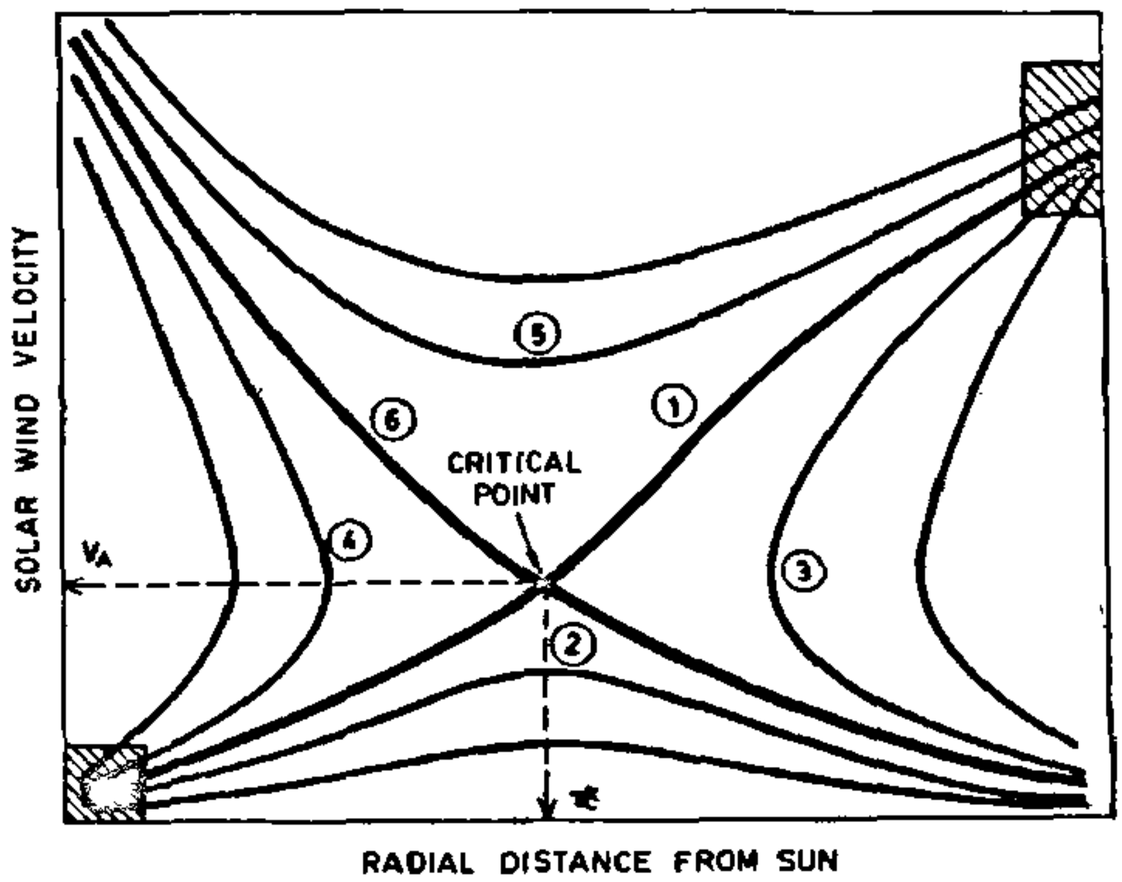

Figure 2. Schematic variations of the solar wind velocity with radial distance from the Sun Different curves depict different solutions of the solar wind equations.

(iii) The supersonic solution is not appropriate as is obvious from the equation of motion, continuity equation and boundary conditions of the problem.

Chamberlain[6] combined the first law of thermodynamics with the equation of heat conduction. Despite assuming that there is no energy deposition, he proposed a solar 'breeze model'. This model yields for $T = 20{,}000$ K and $N_p = 30$ cm^{-3}, the solar wind velocity $V_s = 18$ km sec^{-1}. The curve 1 in Figure 2 shows the transonic nature of the solution of solar wind propagation equation. A critical point is formed by the interaction of curves 1 and 6 defining $V_s = V_A$ for $r = r_c$ as shown in Figure 2. The empirical evidences also show that the realistic solution of solar wind propagation equation in practice connects the two shaded areas at the origin and for $r \to \infty$ and $V_r \to \infty$ as shown schematically in Figure 2. The 'solar breeze' solution is shown by curve 2 in Figure 2 which corresponds to a peak value of V_s at the critical point. Curves 3 and 4 are double valued and hence are unphysical. Similarly, curves 5 and 6 start out as supersonic and therefore are unphysical. Therefore, the 'solar breeze' solutions are not realized in practice and are not consistent with up-to-date measurements.

Two-component fluid model

The conductive heat transport term of a single fluid model contains an implicit assumption concerning the rate of energy exchange between the protons and electrons in the solar wind plasma stream. The radial expansion rate of the solar wind plasma is written as

$$\varepsilon_{exp} = (V_s / N_e)(dN_e / dr). \quad (3)$$

At farther distances N_e varies as $r^{-1/2}$ and the corresponding expansion rate is

$$\varepsilon_{exp} = 2V_s / r. \quad (4)$$

The corresponding energy rate transfer from electrons to solar wind protons is approximated as

$$\varepsilon_E = 10^{-1} N_e T_e^{-3/2} \quad (5)$$

Near the earth's orbit $\varepsilon_E \gg \varepsilon_{exp}$ which implies $T_e \ll 10^3$ K and this temperature is considerably less than the measured proton temperature. In the two-component fluid model of solar wind, the density and velocity of two components must be the same to preserve the local charge neutrality. However, the temperature of the two fluid components of the solar wind can be different[20]. This model of the solar wind is a positive step towards a realistic situation although it gives a three times larger value of N_e and the solar wind velocity is about 50 km smaller than the quiet time mean value of measured solar wind velocity. The solar wind flux conforms to a minimum observed flux.

Solar wind model with magnetic field

The general magnetic field of the Sun and high magnetic field in the sunspot regions play an important role on the dynamics and energy transport through magnetoplasma which finally escapes out into the interplanetary space in the form of general solar wind and high speed solar plasma streams. The solar plasma is fully ionized and is considered to be collisionless and also conforms to a

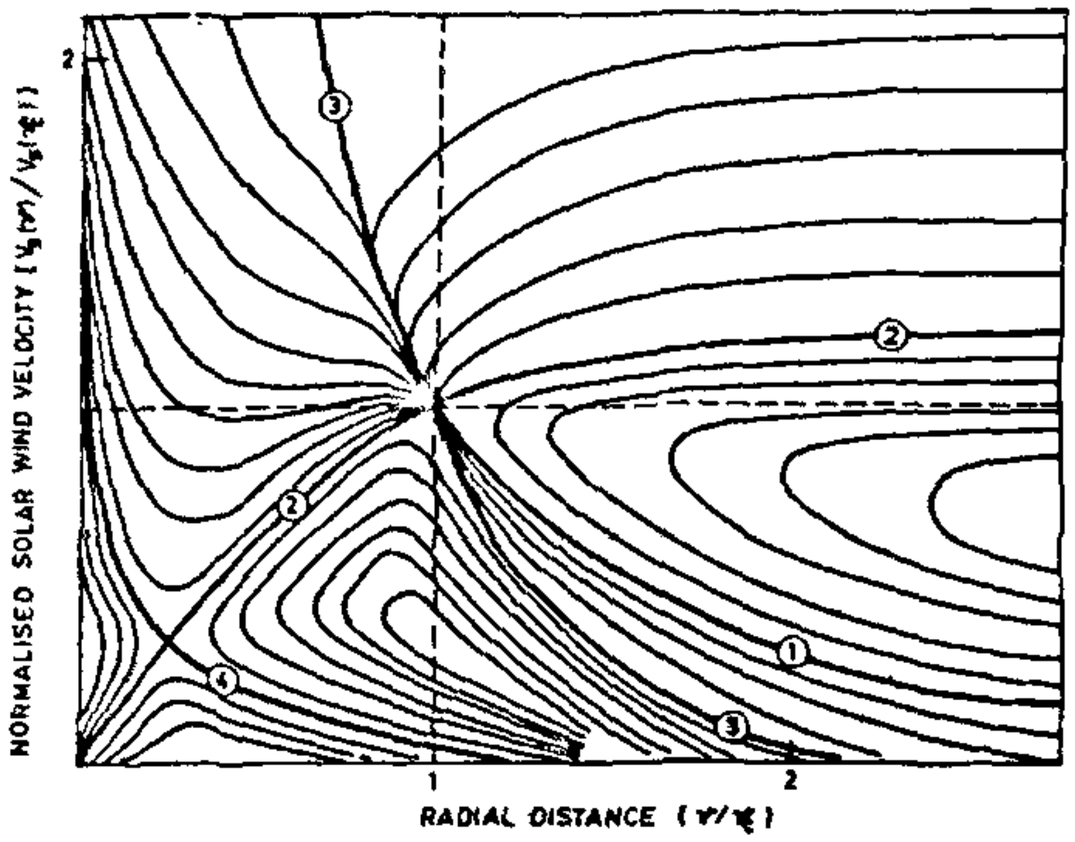

Figure 3. Schematic variation of the solar wind velocity with normalized radial distance from the Sun The modification brought in by the presence of magnetic field is shown

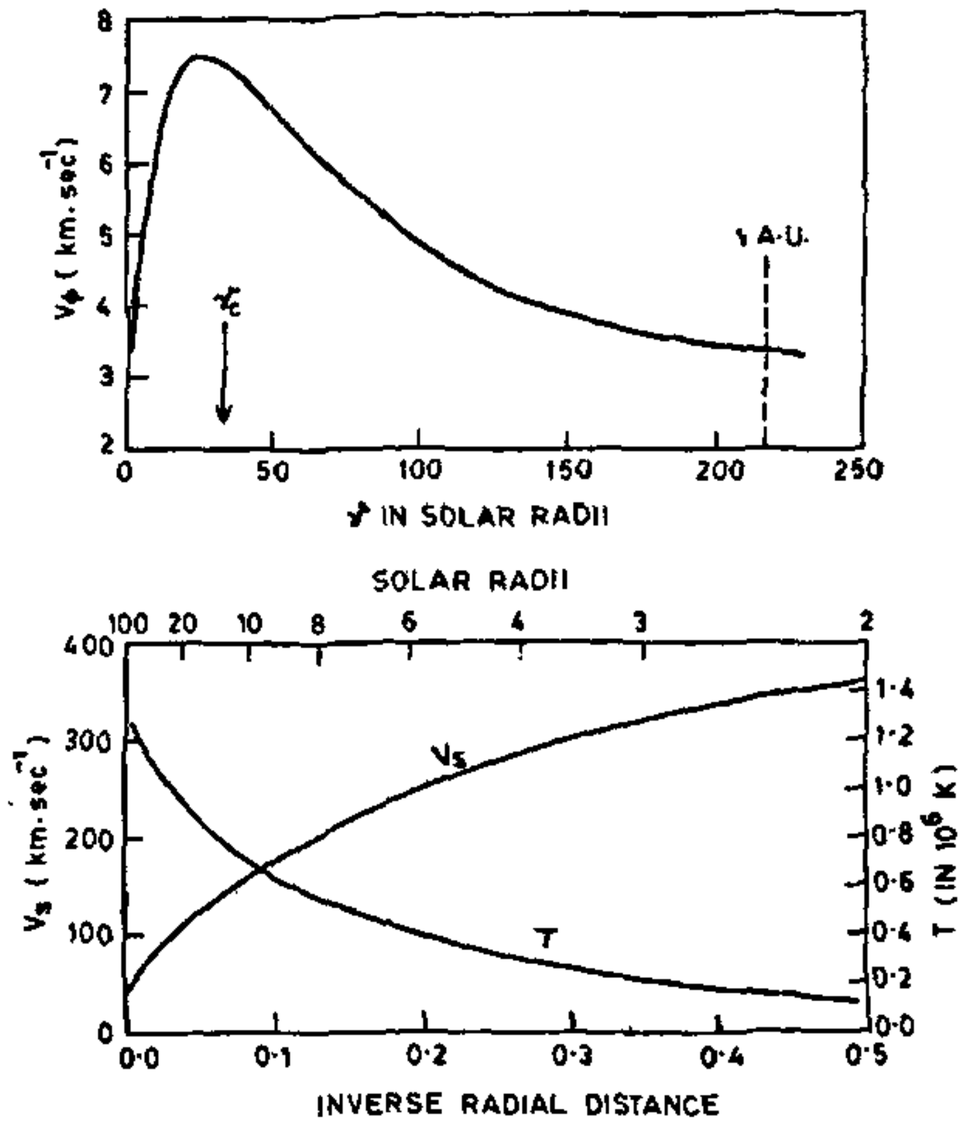

Figure 4. Variation of V_ϕ with distance from the Sun (upper) Variation of solar wind velocity and temperature with radial distance from the Sun (lower).

high plasma conductivity. The convective electric field in the frame of reference moving with solar wind plasma is $(E + V_r \times B) = 0$. The term $(V_r \times B)$ arises from the solar wind frame rotating at a velocity $r\Omega$ and cutting the radially extending solar magnetic field. In this process the $(J \times B)$ force term provides a constant angular momentum per unit mass and helps the escape of the solar wind plasma from the solar corona with a varying angular momentum.

Weber and Davis[21] introduced the polytropic law for energy of the system and computed the variation of normalized parameters similar to that obtained by Parker[22] which is shown in Figure 3. The important features emerging out of their model are:

(i) The curve 1 has an asymptotic velocity of 425 km sec^{-1} and a zero pressure at infinity. Curve 2 also has zero pressure at infinity, but the asymptotic velocity is only 9 km sec^{-1}.

(ii) Curves 3 and 4 have finite pressure at infinity, in contrast to Chamberlain's 'solar breeze' solutions without the magnetic field and zero pressure at infinity.

(iii) Weber and Davis[21] solution was in conformity with the measured values of the solar wind speed near the earth.

(iv) However, this solution does not depict the situation of high temperature solar coronal conditions and low charged particle density.

Brandt *et al.*[23] considered full energy equation in place of polytropic energy equation and extended the work of Weber and Davis[21]. The solutions near the earth $r > 2\ R_s$ are shown in Figures 4 *a*, *b* and these figures correspond to:

$N_e = 6\ cm^{-3}$,

$V_r = 315\ km\ sec^{-1}$,

$V_\phi = 2.5\ km\ sec^{-1}$ and

$T = 3.25 \times 10^5\ K$.

These values are reasonable for a quiet solar wind condition, however, this model does not reveal the solar wind parameters that are typical of solar active region conditions.

Effect of realistic coronal conditions on solar wind

The properties of solar wind generation and propagation discussed so far are highly idealized as being time-independent and having spherical symmetry. However, it is well known, that any realistic model of solar wind should account for inhomogeneities of plasma flow, magnetic field changes and also changes in the localized flare conditions, resulting into longitudinal variations in the solar wind velocity.

In the presence of high and low solar wind speeds that invariably exist in practice, the collision of the solar plasma at relative velocity $(V_h - V_L)$ occurs. If the colliding velocity $(V_h - V_L) > V_{ma}$, the magneto-acoustic

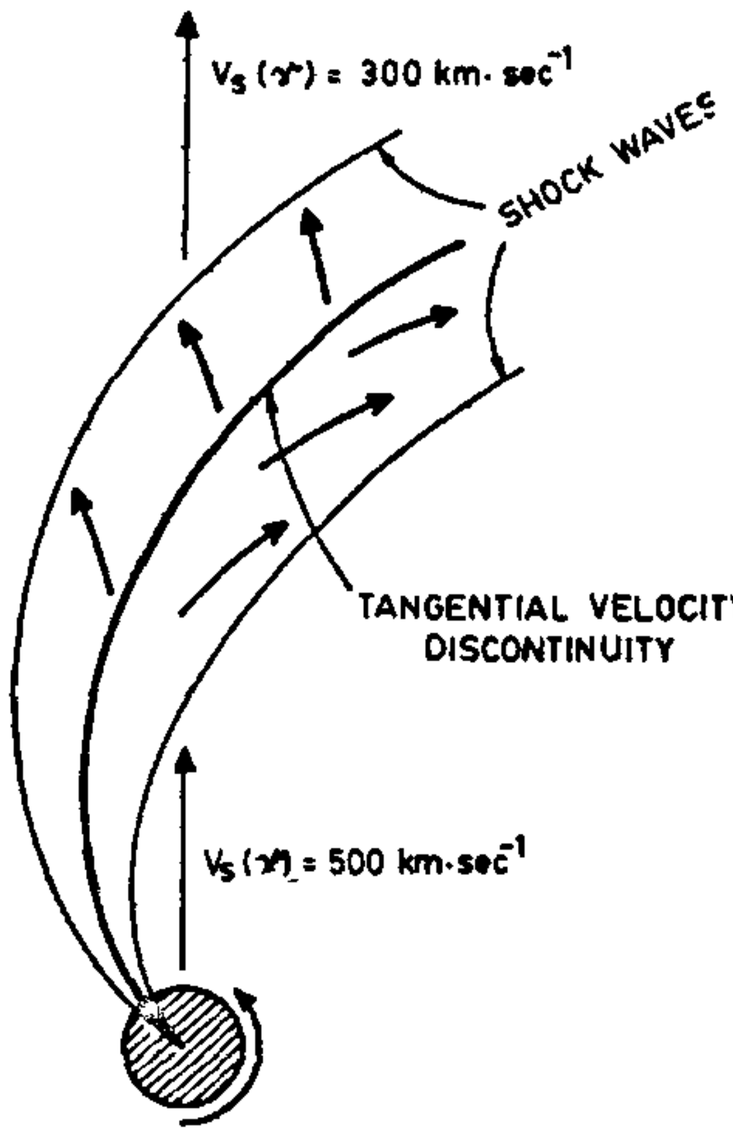

Figure 5. Schematic diagram showing formation of contact surface near the target arising from the non-uniform flow of solar wind

velocity, a double shock layer is formed that is separated by a tangential velocity discontinuity as shown in Figure 5. The plasma flow direction is differentially deviated in the shocked region which forms a tangential velocity discontinuity. This region is unstable and once formed may co-rotate for several solar rotations. The co-rotation phenomenon is associated with longitudinal velocity gradient in the solar wind velocity and is ascribed to a typical M-region formation on the solar surface.

The solar flares are characterized by build-up and decay processes of magnetoplasma in which the solar corona is further heated up. It is well known that there are no stationary solutions when the solar corona is heated above a critical value. Under such conditions a blast wave is formed which propagates into the interplanetary medium. The magnetic field structure in the blast wave is shown schematically in Figure 6. The blast wave consists of quiet solar wind swept up by the momentum of the blast wave and is found to account for the mass loss in the solar wind. The dissipation of blast wave at large distances from the Sun is known to result into increase of electron temperature.

Solar coronal holes and the solar wind

In addition to the development of steady state co-rotating solar wind models, the simultaneous observations of optical, X-rays, microwave fluxes and the

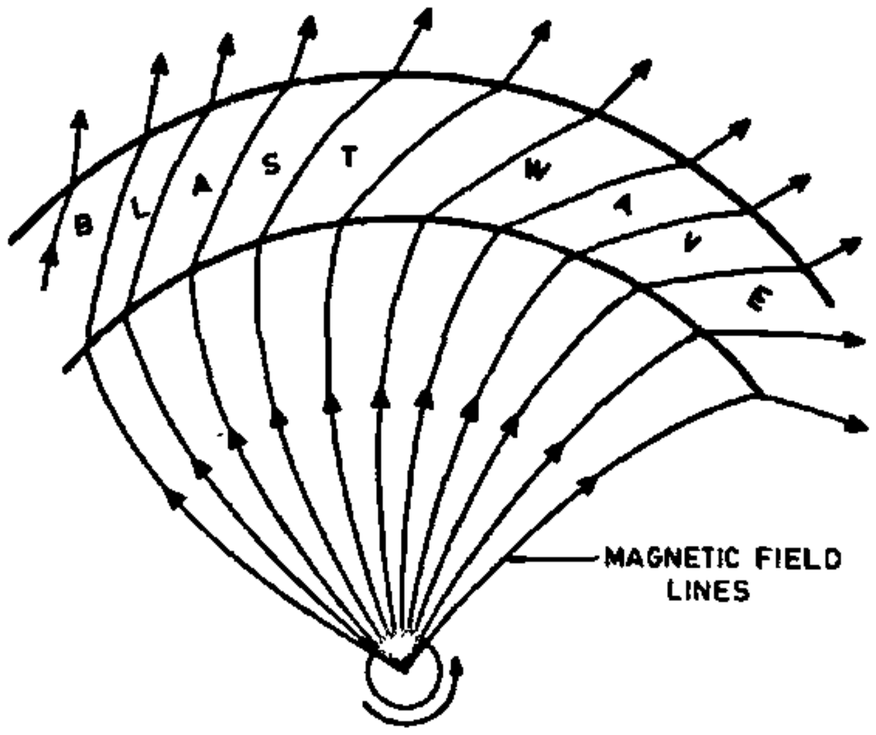

Figure 6. Magnetic field structure in the interplanetary blast wave

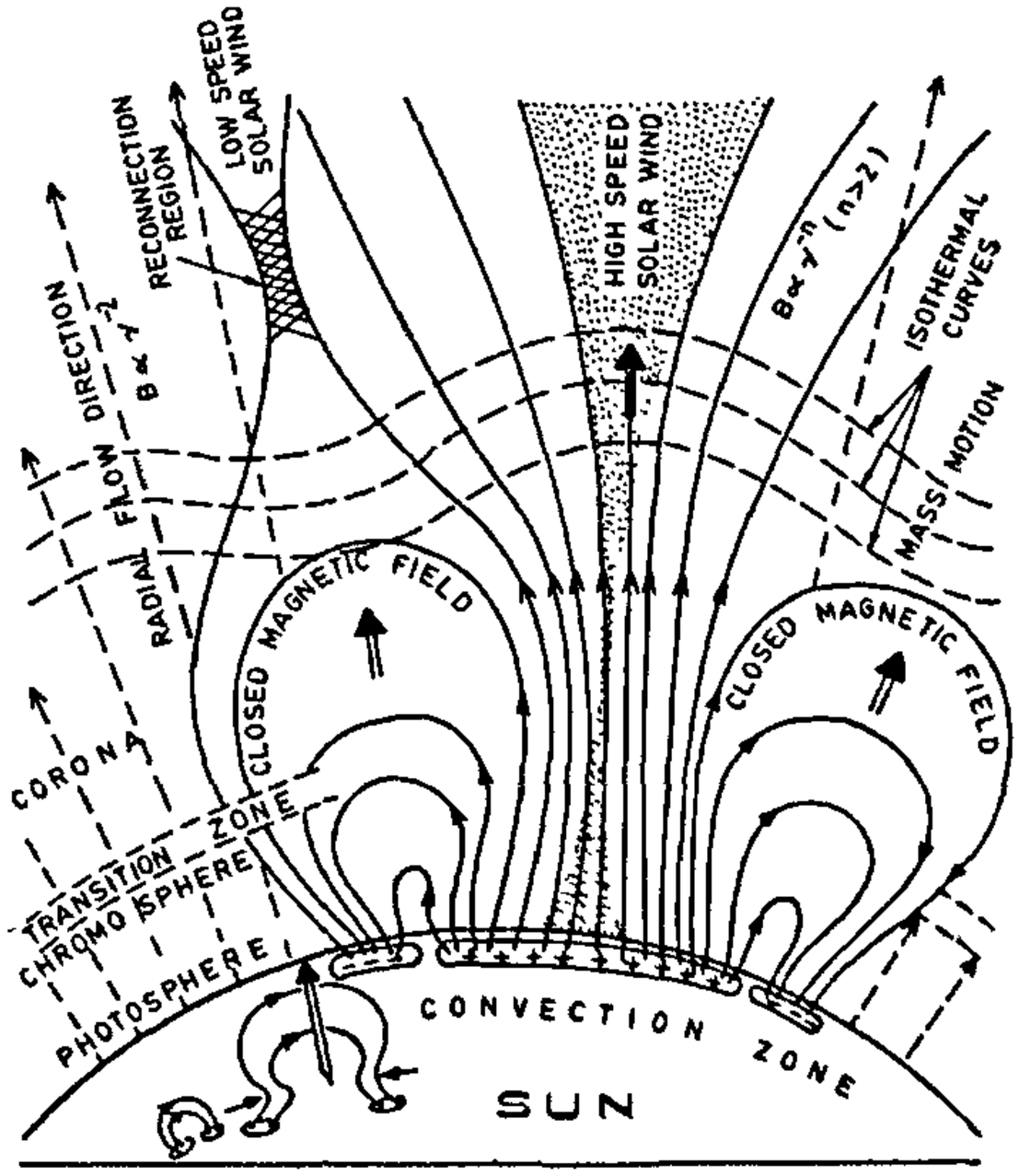

Figure 7. Schematic showing strong and weak solar wind emissions from different parts of solar corona and coronal holes

solar wind velocity and proton fluxes have provided important clues regarding generation and propagation of solar wind. A schematic model of solar wind emission from the coronal hole region has gained general acceptability. The systematic development of a bi-polar sunspots pair is shown which forms adjacent helmet-like magnetic field structure as shown in Figure 7. Between the two closed loop magnetic field structures, the magnetic fields are oppositely directed and form a thin

neutral current sheet. The magnetic field tends to merge at a point and on either side of this merging region, the magnetic field configuration becomes divergent. The protons moving upwards from the transition zone region are continuously accelerated in the divergent magnetic field region acquiring additional energy. The isothermal curves are shown by the dotted lines in Figure 7. The closed field structures correspond to higher temperatures, whereas, the opened magnetic field region correspond to a net lower temperature characterized by lower optical emission regions that are known as 'coronal holes'. The radially accelerated solar wind plasma stream is emitted from the solar coronal holes. The closed magnetic field regions correspond to energetic protons and electrons injected inward into the denser regions of the corona, and the chromosphere. The closed magnetic field regions also correspond to much weaker solar wind transmitted into the interplanetary space. The optical, X-rays and microwaves are known to be generated in the inner coronal regions. The simultaneity and correlations of experimentally measured data have been carried out extensively and some of these features have provided important tool for diagnostic study of solar wind-generating processes and the solar wind propagation features. The indirectly probed parameters of solar wind are known to be in good agreement with the directly measured solar wind parameters under normal conditions.

The coronal holes with a divergent magnetic field contain greater magnetic flux per unit area compared to regions with closed magnetic field configurations. According to Svalgaard *et al.*[24] about half of the open magnetic flux is contained in the polar coronal holes during moderate solar activity. It is well-known that during the solar activity minimum, the coronal holes lie in the polar regions and their area coverage becomes maximum. On the other hand the cross-sectional area of equatorial coronal holes is small and the solar wind flux enhances. Assuming steady state charged particle solar wind flux by $n_0 v_0$, the high speed solar wind flux from coronal holes is written as

$$nV_{Sh} = n_0 V_{S0} \left[\frac{r}{R_S}\right]^2 \left[\frac{1-S_{CH}}{1-f\,S_{CH}}\right], \tag{6}$$

where S_{CH} is the total area of coronal holes expressed in terms of solar surface and f is the divergence factor of magnetic field in the coronal holes. The particle flux density at the base of the coronal hole does not change the strength of the magnetic field and field divergence factor only affects the solar wind particle flux nv_S. The strength of the magnetic field in the coronal hole region during the solar activity maximum period is substantially greater compared to the magnetic field strength during solar activity minimum period. The divergence factor of coronal hole magnetic field is expressed as[25]

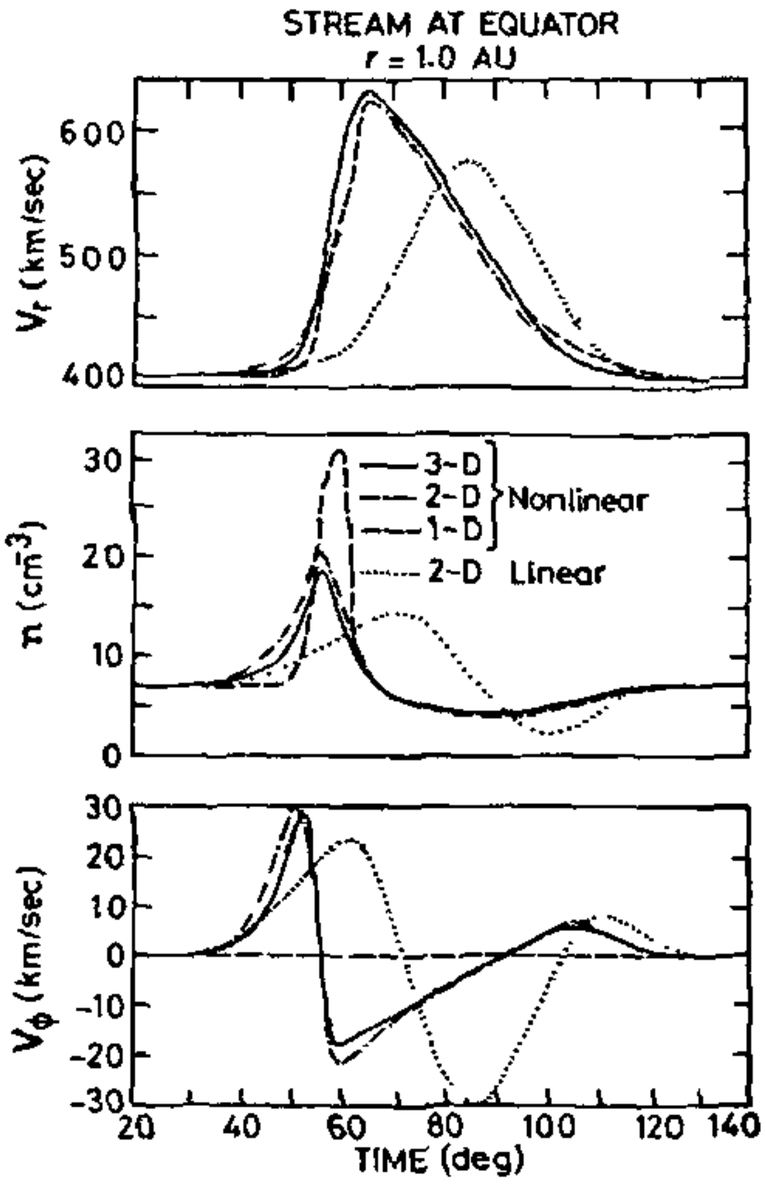

Figure 8. Variation of solar wind flux density nv_S with solar activity year during 1972 to 1983 for solar wind stream velocity $V_S > 500$ km sec^{-1} and $V_S < 400$ km sec^{-1}

$$f = \frac{B_{CH}}{B_r}\left[\frac{R_S}{r}\right]^2, \tag{7}$$

where B_{CH} is the magnetic field at the base of coronal hole in the photospheric region and B_r corresponds to a distance r from the solar surface. The variations nV_S corresponding to high speed and low velocity solar wind over a solar cycle are shown in Figure 8. The nature of variation of nV_S associated with $V_S > 500$ km sec^{-1} and $V_S < 400$ km sec^{-1} shows decreasing and increasing trends during 1973 to 1977 and thereafter becoming almost equal as shown in Figure 8. This behaviour of nV_S is averaged over the entire solar surface. Just before the solar activity maximum year 1978, the coronal hole area in the polar region decreased and almost vanished during the year of magnetic polarity reversals in the polar magnetic field. Thus, we find that the solar wind flux plays an important role in its interactions with planetary atmospheres, moons and comets. The nV_S has been found to decrease in the area of polar coronal holes and they disappear prior to the appearance of maximum solar activity. The coronal holes appear again during the declining phase following the polarity reversal of the polar magnetic field and formation of polar coronal holes.

Three-dimensional model of co-rotating solar wind

The large scale plasma inhomogeneities in the solar corona expand with high speed and couple with the solar rotation to produce significant longitudinal alignments of solar wind particle flux in the interplanetary space. The solar rotation resulting into a spiral structure of solar magnetic field introduces a basic anisotropy in the solar wind propagation properties. The azimuthal solar wind speed gradients are directly driven by the solar plasma stream interaction with planets while the meridional solar wind speed gradients generally arise as a consequence of solar magnetic field and solar rotation-induced latitudinal variations in the solar coronal plasma expansion. A number of studies have given detailed information about the solar wind flow, including the effects of embedded magnetic field and solar rotations. The one-dimensional (1-D) and two-dimensional (2-D) studies of solar wind have clearly shown the effect of magnetic field on shock formation[26–29]. The 2-D modelling of solar wind is appropriate in the neighbourhood of the solar equatorial plane in the absence of local latitudinal gradients in the speed of expanding solar coronal plasma. The 3-D modelling has been carried out by Pizzo[30]. This study is essentially numerical hydrodynamic modelling which accounts for global and co-rotating evolution of solar wind in the interplanetary space. With simple modifications this 3-D model can be easily reduced to 2-D and even 1-D descriptions. Pizzo[30] has computed the radial velocity, azimuthal velocity and density of solar wind stream in the equatorial plane at 1 AU that are shown in Figure 8. The results of 2-D linear model obtained by Siscoe and Finely[31] are shown by the dotted curves in Figure 9. The boundary conditions used by Pizzo[30] for 3-D modelling are hypothetical in nature. However, in general, the results of 3-D modelling hold good for a broad range of solar wind structures. The flow is rather heavily momentum-dominated, which limits its potentiality to exhibit real dynamical situations at farther distances from the source region. The 3-D model of solar wind propagation was further improved by Pizzo[32, 33]. In particular, the effect of spiral magnetic field on the evolution of co-rotating solar wind has been worked out. It was shown that the secondary large-scale phenomena are associated with the 3-D solar wind streams. Further improvements over this model have been reported, however, the reported claim of improvement in the model cannot be checked from the available *in situ* measurements.

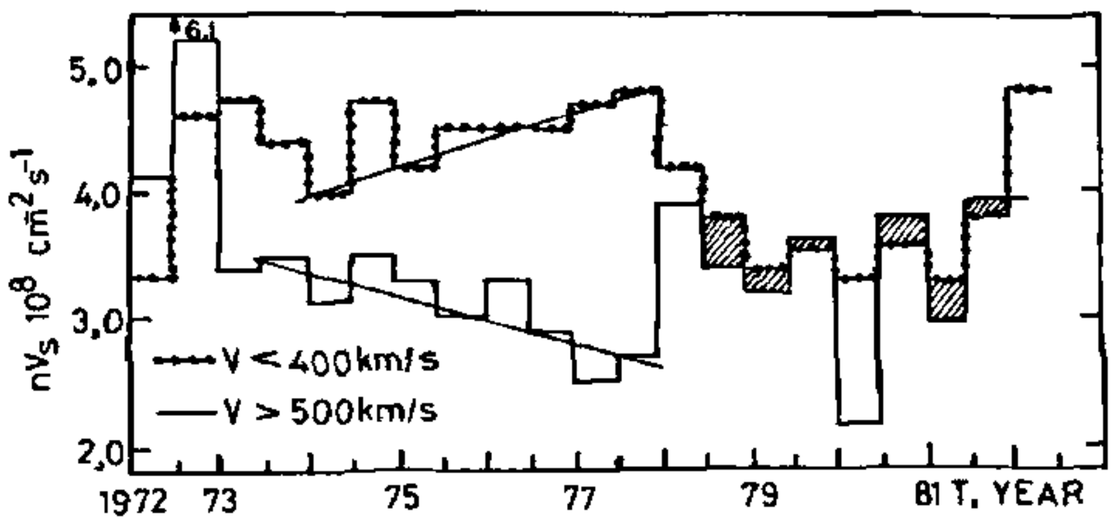

Figure 9. Variation of solar wind velocity components and proton density with time at 1 AU corresponding to 2-D linear model and 1-D, 2-D and 3-D nonlinear models.

Solar wind interaction with planetary atmospheres

Various aspects of solar wind generation and propagation have been discussed. One of the basic aims of knowing these details is to study the outcome of the solar wind interaction with the planetary atmospheres in the dayside and nightside. It is well known that the solar wind interacts with the magnetic and non-magnetic planets quite differently and gives rise to typical morphological features. The solar wind interaction with earth's magnetosphere is typical of magnetic planets. The solar wind is stopped at a large distance forming a magnetopause on the dayside and bending of solar wind around the planets results into an extended magneto-tail on the nightside. In the case of non-magnetic planets, the solar wind is able to penetrate very close to the planet. The solar wind picks up the photoionized and charge-exchanged interplanetary ions that also move with the solar wind protons. The solar wind is consequently mass-loaded which results into piling-up of the solar magnetic field. The thin region with steep electron density gradient is formed on the dayside of the non-magnetic planets which is known as 'ionopause' region in contrast to that of 'magnetopause' in the case of magnetic planets. Mars behaves exactly the same way as Venus does and the phenomena of mass-loading and formation of ionopause are well known. The solar wind interaction and the nature of solar wind plasma around the planet depends greatly on the size of the planetary and cometary obstacles. Recently, the *in situ* studies of solar wind and Halley Comet have been carried out[34]. The interaction of solar wind with comets, in general, and Comet Halley, in particular, has been carried out and interaction details have been studied theoretically and simulated using various interaction models. These studies have shown that the interactions are Venus-like which forms a barrier very close to the dayside region of the comets. The barrier region in the case of comets is small in size and was named as 'Cometopause' by Gringauz[35].

In addition to bow shock formation, mass-loading and barrier region formation, the solar wind loses a part of its energy which goes into heating of the ionosheath of the non-magnetic planets[36, 37]. The formation of current sheet and reconnection phenomena giving rise to neutral

points result into acceleration of charged particles. A fraction of these charged particles is trapped by the magnetic field which finally precipitates and gives rise to auroral display in the polar regions of the magnetic planets. The auroral phenomena do not occur in the non-magnetic planets. Aurora-like optical emissions have been observed aboard PVO and these optical radiations observed in the nightside of Venus is attributed to an altogether different mechanism.

Concluding remarks

The solar wind generation and propagation processes are important for a detailed study of planetary atmospheric, ionospheric and magnetospheric phenomena in general. In the case of earth, the role of solar wind has been extensively studied and there are still, many unsolved problems. The effect of solar wind on the inner planets such as Mercury, Venus, Mars, their moons and comets plays a much more important role. Mercury is much closer to the Sun having a very thin atmosphere but significant magnetic field. The solar wind interaction with Mercury is known to form a well-developed magnetosphere with a negligibly thin ionosphere. The theoretical and *in situ* studies of Venus and Mars have shown the formation of low altitude ionopause and an extended ionotail. The behaviour of Mars and Venus atmospheres is illustrative of the solar wind response to non-magnetic planets and also provide an important clue for solar wind interaction with planetary moon and comets. Cometary interaction with solar wind provides new information about the small and thick magnetopause region on the dayside. The Cometotail is now known to provide a special feature hitherto unknown in the case of planetary tails either in the case of magnetic or in the case of non-magnetic planets. The detailed knowledge of solar wind emission, propagation and mass-loading is important to decipher newer features of solar wind interactions with different targets.

1. Chapman, S. and Bartel, J , *Geomagnetism*, Oxford University Press, Clarendon, 1940
2. Biermann, L., *Z. Astrophys (FRG)*, 1951, **23**, 265
3. Biermann, L , *Observatory (UK)*, 1957, 77, 109
4 Parker, E N , *Astrophys J* , 1958, **128**, 664
5. Chapman, S , *Proc R Soc London*, 1959, **253**, 450
6 Chamberlain, J W., *Astrophys J* , 1961, **133**, 675
7. Chamberlain, J W , *Astrophys J* , 1965, **141**, 320
8 Holloweg, J V., *Astrophys J* , 1973, **181**, 547.
9. Holloweg, J V , *Res Geophys* , 1978, **16**, 689
10 Holloweg, J. V , *Sol. Phys (Netherlands)*, 1981, **70**, 25
11. Vanbeveren, D. and de Loore, C , *Sol Phys* , 1976, **50**, 99
12. Couturier, P., Mangeney, A and Souffrin, P , *Astron Astrophys* , 1979, **74**, 9
13 Souffrin, P., *Astron Astrophys* , 1982, **189**, 205
14. Bohlin, J. D , *Coronal Holes and High Speed Solar Wind* (ed Zirker, J B), Colorado Associated University Press, USA, 1977, p 27
15 Hundhausen, A. J , *Coronal Holes and High Speed Solar Wind* (ed Zirker, J B), Colorado Associated University Press, USA. 1977, p 148
16. Zirker, J B , *Rev. Geophys* , 1977, **15**, 237
17. Holtzer, T. E. and Leer, E , *J Geophys Res* , 1980, **85**, 4665
18. Olbert, S , *Solar Wind V*, NASA Conf Pub , 1983, CP-2280, p 149
19 Scudder, J. D and Olbert, S , *Solar Wind V*, NASA Conf Pub , 1980, CP-2280
20. Hartle, R E and Sturrock, P A., *Astrophys J* , 1968, **151**, 1155
21. Weber, E J and Davis, L., *Trans Am Geophys. Union*, 1967, **48**, 217
22. Parker, E N , *Space Sci. Rev* , 1965, **4**, 666
23. Brandt, J. C., Wolf, C. and Cassinelli, J. P , *Astrophys J* , 1969, **156**, 117.
24 Svalgaard, L., Duval, T. L. and Scherer, P H , *Sol Phys* , 1978, **58**, 225.
25. Kovalenks, V. A., *Planet Space Sci.*, 1988, **30**, 1343
26. Nakagawa, Y and Wellck, R E , *Sol Phys* , 1973, **32**, 257
27 Steinolfson, R S , Dryer, M. and Nakagawa, Y , *J Geophys* , 1975, **80**, 1223
28 Steinolfson, R. S and Tandberg-Hansen, E , *Sol Phys* , 1977, **55**, 99
29. Han, S M , PhD Thesis, University of Alabama, Huntsville, 1971
30 Pizzo, J V , *J Geophys Res* , 1978, **83**, 5563
31. Siscoe, G L. and Finely, L T., *J Geophys Res* , 1972, **77**, 35
32 Pizzo, J. V., *J Geophys Res* , 1980, **85**, 727
33 Pizzo, J V., *J. Geophys. Res* , 1982, **87**, 4347
34 Special volume reporting various *in situ* measurements *Nature*, 1986, **321**, No 6067.
35 Gringauz, K L., *Nature*, 1986, **321**, 269
36 Gombosi, T. I , Crevens, T E , Nagy, A F , Elphic, R C and Russell, C. T , *J. Geophys Res* , 1980, **85**, 7747
37 Crevens, T E , Gombosi, T. I , Kozyra, J , Nagy, A F and Brace, L. H , *J Geophys Res* , 1980, **85**, 7778